Korean J. Chem. Eng., **29**(10), 1373-1381 (2012)
DOI: 10.1007/s11814-012-0063-7

A dynamic adsorption model for the gas-phase biofilters treating ethanol: Prediction and validation

Eun Ju Lee and Kwang-Hee Lim†

Department of Chemical Engineering, Daegu University, Kyungsan, Gyeongbuk 712-714, Korea
(*Received 14 November 2011 • accepted 14 May 2012*)

Abstract−A dynamic adsorption model was proposed using the lumping process for an adsorption system. This novel approach uses a four-component structure model: gas phase, enclosed aqueous phase, sorption volume and porous media surface adsorption. A clouding effect represented by k_a (dynamic adsorption constant) was adopted to explain the adsorption process. The clouding effect assumes that the adsorption rate is decreased as the adsorption sites on the media surface are occupied. In the equilibrium stage the Freundlich adsorption isotherm was adopted. The proposed dynamic adsorption model was then predicted in comparison with the experimental data of an adsorption-column to estimate adsorption model parameter values in a biofilter fed with ethanol at 4,100 mg ethanol/m^3 (or 2,000 ppmv). Model validation was performed for the adsorption column fed with ethanol at 2,050 mg ethanol/m^3 (or 1,000 ppmv). Results showed that the mechanistic model was able to simulate the dynamic behavior of an adsorption process successfully according to the corresponding adsorption experimental data.

Key words: Dynamic Adsorption Model, Process Lumping, VOC, Model Prediction

INTRODUCTION

The growing demand for biofilters leads to the necessity of basic design such as biofilter design and scale-up and industrial needs on conceptual understanding of biofilter operation, which makes us investigate and develop biofilter modeling. Previous works describe the steady-states or can be applied to a narrow range of operating conditions [1-6], and others describe the transient performance of a biofilter [7-14]. Our future goal is to establish the pressure-drop model of a biofilter, in terms of a modified pore network model or Ergun equation, in which a void fraction of a biofilter may be an important factor. Its void fraction is strongly correlated with the rate of microbial growth related to the substrate concentration in a biofilm. Determining the pool size of adsorption on the biofilter media, the substrate concentration in a biofilm may be estimated in terms of conserved mass balance considering its microbial degradation. Therefore, it becomes necessary to predict the dynamic behavior of adsorption on biofilter media under the same conditions as those of a biofilter-operation. In a biofilter, moisture is continuously provided through the pre-humidification of the inlet gas stream because moisture content of the filter bed is a critical factor for the successful operation of a biofilter. The relative humidity of the inlet gas stream is even raised above 99 percent for the optimum performance of biofilters [15]. Lith [16] and Auria et al. [17] suggested the moisture content in a biofilter medium be between 40% and 60% by wet weight for its optimum sustained performance. As a result of normal biofilter operation, the pore space is filled with a condensed aqueous phase and the bare solid surface of a biofilter medium is still covered with an aqueous layer even though there are patches of biofilm on the solid surfaces on the medium. Thus, it is not realistic that a dried bare solid/air interface without liquid layer exists in the normal performance of a biofilter. This leads one to construct a dynamic adsorption model for the media of biofilter design, which is assumed to be enclosed with an aqueous layer.

Joly and Perrad [18] used linear driving force approximation associated with various adsorption isotherm characteristics for the dynamic adsorption of volatile organic compound traces by porous adsorbent beds. Gholami et al. [19] developed mathematical modeling of gas dehydration using an adsorption process, in which a parametric study was performed to clarify the effects of different operational parameters. Zhang et al. [20] develop a dynamic adsorption model under constant-pattern wave conditions to predict the breakthrough behavior of trichlorofluoromethane adsorption in a fixed bed packed with activated carbon fibers. However, their dynamic adsorption models have been based upon very conventional governing equations of typical adsorption process.

In this paper, the proposed adsorption model consists of four model-components: gas phase, enclosed aqueous phase, sorption volume and adsorption surface in the pore of media. It describes the dynamic behavior of the adsorption column operated under the condition of almost saturated relative humidity of waste air fed to the biofilter, to treat waste air containing such a VOC as ethanol. The proposed dynamic adsorption model is then fitted to the experimental data of the adsorption-column to estimate adsorption model parameter values in a biofilter. The parameters of the proposed adsorption model are estimated, using the values of Freundlich adsorption isotherm constants obtained from the adsorption isotherm data [21], by not only parametric sensitivity analyses but also subsequent qualitative analyses with the dynamic adsorption experimental data [22] from the operation of an adsorption column. The dynamic adsorption behavior is predicted using the proposed adsorption model with the estimated values of the model parameters. Then the predicted dynamic adsorption behavior is compared with the dynamic adsorp-

†To whom correspondence should be addressed.
E-mail: khlim@daegu.ac.kr

tion experimental data, by which the proposed adsorption model is validated.

EXPERIMENTAL

1. Dynamic Continuous Adsorption Experiment

An adsorption column was manufactured in a way that a feed gas entered at the top of the adsorption column composed of two acryl tubes (diameter: 5 cm, length: 25 cm) connected in series. Upper and lower reactor tubes were packed up to 22 cm and 22 cm from their bottom with media, respectively, so that the total effective height of the adsorption column was adjusted to 44 cm. Among the four sampling ports of the adsorption column, the first and second were positioned 14 cm below top the surface of the upper media and 14 cm below the top surface of the lower media, respectively. The remaining two sampling ports were positioned at the entry and exit points of the adsorption column. Therefore, the ratios of effective height to total were 0.0, 0.3, 0.8 and 1.0 for the sampling ports at entry, first, second and exit, respectively. In the adsorption column, the mixture of equal volume of granular activated carbon (GAC) sterilized at 100 °C in dry-oven and compost sterilized in autoclave at 121 °C for 15 min with the average radius of 3 mm and 0.6 mm, respectively, was used as the packing media. The characteristics of the adsorbent packed in the adsorption column are shown in Table 1. Air provided by the blower (Young Nam Yasunnaga, outlet pressure; 0.12 kg/cm^2, maximim flow rate; 43 L/min) passed through a series of three humidifier columns maintained at 40-50 °C by thermostat (Jeil Science, J-PW B2) and its relative humidity was maintained at 95-99%. The adjusted amount of ethanol was continuously injected by syringe pump (KD Scientific, Model: KDS200) into a heated conduit of 140 °C through which humidified air passed. Waste-air containing ethanol of a set concentration was artificially manufactured in this way and was provided to the top of the adsorption column. From time to time the relative humidity of the feed gas was measured to maintain >90% relative humidity. A tygon tube was used to convey pure air, and a viton tube was used to transport manufactured waste-air containing ethanol as feed gas to the adsorption column. The temperature of the adsorption column was maintained near 30 °C by a heating band and temperature controller, and Swagelok was used for all fittings. The schematic diagram of dynamic-continuous flow-adsorption process is in Fig. 1. In the first and second experiments, feeding air containing ethanol of 1,000 ppmv (or 2,050 mg ethanol/m^3) and 2,000 ppmv (or 4,100 mg ethanol/m^3), respectively, was supplied to the adsorption system at the rate of 2 L/min. Their dynamic adsorption behaviors were observed until it reached isothermal adsorption equilibrium.

Table 1. Characteristics of the media packed in the adsorption column and used for adsorption isotherm experiments

	GAC	Compost	GAC/compost
Density (g/cc)	0.41	0.37	0.39
Moisture content (%) under wet condition	45	62	54
Wet porosity	0.553	0.702	0.602
Equivalent diameter (mm)	2.5	0.6	-
Interfacial area per unit volume (m^2/m^3)	1292.6	2980	2136.3

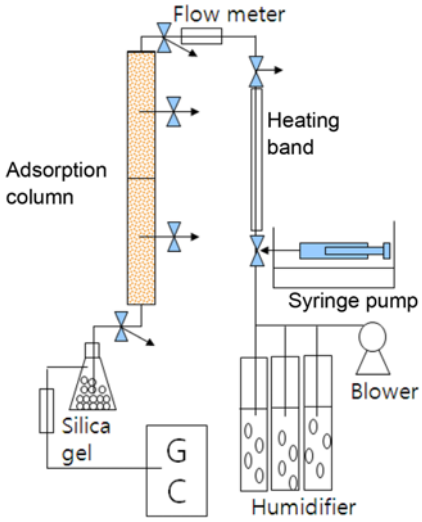

Fig. 1. Schematic diagram of dynamic-continuous flow-adsorption process.

PROPOSED DYNAMIC ADSORPTION MODEL

1. Adsorption Model Formulation

In formulating an adsorption model the following are assumed:

1) The mass transfer resistance in the gas-phase is negligible, compared to that in the aqueous phase.

2) The aqueous film thickness (l) is much smaller than the diameter of packing particles (medium) so that the aqueous film covering each granular adsorbent may be treated as a planar surface.

3) Substrate transport through the aqueous film and into the sorption volume filled with the aqueous phase is made by diffusion.

4) The interface between the gas phase and the aqueous film is in the equilibrium.

5) No catalytic reaction except for adsorption and desorption on the surface of the medium (beneath the aqueous film) exists upon the adsorption of the organic components.

6) The adsorption column is treated as a plug flow reactor.

Fig. 2 shows the schematic diagram of the adsorption model where the aqueous film is treated as a planar surface as stated in the assumption. With the above assumptions, the differential equations for the concentration profile of a dissolved organic component (C_l) in the aqueous film can be described as:

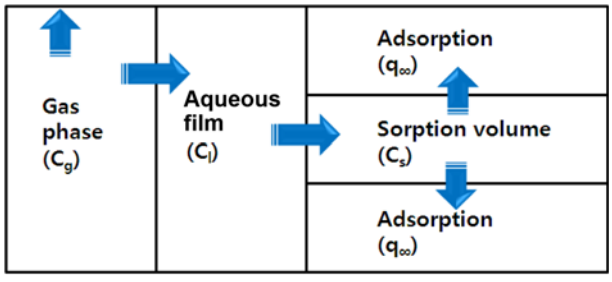

Fig. 2. Schematic diagram of adsorption model.

$$\frac{\partial C_l}{\partial t} = D_e \frac{\partial^2 C_l}{\partial x^2} \tag{1}$$

where D_e is a diffusion coefficient in the aqueous film.

The proposed boundary condition at the interface between the gas phase and the aqueous film for the governing equation is:

$$C_l(t, x=0) = \frac{C_g(t, h)}{m} \tag{2}$$

where m is a distribution coefficient between the gas phase and the aqueous film.

One may assume that the dissolved organic concentration in the sorption volume filled with aqueous phase, of the medium (C_s) is uniformly distributed and is continuous at x=*l*, which leads to another boundary condition of $C_l(t, x=l)=C_s(t)$. The mass balance in the sorption volume of the medium is described as below:

$$\frac{V_{sorption}}{V}\frac{dC_s}{dt} = -D_e \frac{\partial C_l(t, x=l)}{\partial x} a - k_a(1-\varepsilon)C_s \tag{3}$$

where k_a is the adsorption rate constant with excess adsorption capacity, that is proportional to the adsorption area per unit volume of adsorbent and a, V, $V_{sorption}$ and e are the interfacial area of an adsorbent between gas and aqueous phases per unit working volume of an absorption column, absorption column-bed volume, sorption volume and bed porosity, respectively.

Adsorbents can either diffuse in the adsorbed state along the pore surface (surface diffusion) or within the fluid contained in the pores (pore diffusion). Since the former prevails over the latter in actual adsorption phenomena [23-25], the process of the surface diffusion is lumped in the term of adsorption in the right-hand-side of Eq. (3). The surface diffusion coefficient of granular activated carbon (GAC) is ca. 10^{-15} m^2/sec [23-25] and much less than the ethanol-water diffusion coefficient, D_e, in the aqueous film (1.28×10^{-9} m^2/sec [26]). Under the circumstances, the ethanol diffusion process in GAC is substantially slower than the diffusion process through the aqueous film. Hence one can deal with Eq. (3) in such a quasi-steady state that the diffusion flux through the aqueous film is generated as soon as the diffusion inside the medium (sorption volume) occurs.

Therefore, the boundary condition at the interface between the aqueous film and the sorption volume of the medium, filled with aqueous phase is formulated by lumping the processes of adsorption as well as diffusion, as:

$$\frac{\partial C_l}{\partial x}(t, x=l) = -\alpha C_l(t, x=l) \qquad \text{where } \alpha = \frac{k_a(1-\varepsilon)}{D_e a} \tag{4}$$

2. Steady State Solutions with Excess Adsorption Capacity

$$0 = D_e \frac{d^2 C_l}{dx^2} \tag{5}$$

with the boundary conditions of Eqs. (2) and (4). By solving Eq. (5), one obtains:

$$\frac{C_l}{C_g/m} = \frac{1+\alpha l(1-\sigma)}{1+\alpha l} \tag{6}$$

where σ(*i.e.*, x/*l*) is the dimensionless coordinate in the aqueous film thickness.

As in Fig. 1, the differential mass balance in the gas phase may be formulated as below.

$$\varepsilon \frac{\partial C_g}{\partial t} + u \cdot \frac{\partial C_g}{\partial h} = -Na \tag{7}$$

where $N = -D_e \left.\frac{\partial C_l}{\partial x}\right|_{x=0}$ and a and u denotes the interfacial area per unit volume of the fixed bed and approach velocity of the waste air stream, respectively.

From Eq. (6), N for the steady state of C_l becomes:

$$\frac{D_e C_g}{m}\frac{\alpha}{1+\alpha l} \tag{8}$$

Substituting Eq. (8) into Eq. (7), one may obtain the solution for steady state as below:

$$\frac{C_g}{C_{go}} = e^{-N_r \zeta} \tag{9}$$

where ζ, C_{go} and N_r are the dimensionless height of the adsorption column, the concentration of untreated inlet waste gas and ($HD_e a$/um)(α/(1+αl)), respectively.

It is noteworthy that with α=0, C_g becomes C_{go}.

3. Dynamic Adsorption Model with a Limited Adsorption Capacity

Eq. (3) is generally assumed to be in a quasi-steady state since the order of magnitude of the period for the organic pollutant to pass through the aqueous film, whose maximum thickness is assumed to be 100 μm, is ca. 10 s according to the approximation of (l^2/D_e)= ($(10^{-4}\ m)^2/(10^{-9}\ m^2/s)$).

In modeling the transient behavior of an adsorption column, the clouding effect is applied to k_a in order to explain that as an adsorption proceeds, the occupancy of adsorption sites results in the decreased adsorption velocity and to consider the reversible adsorption process. When the clouding effect is applied to show the decreased adsorption rate as adsorption proceeds, k_a is no longer a constant but assumed to decrease in the way that it does in Eq. (10). Thus in the boundary condition of Eq. (4) k_a can now be expressed as below.

$$k_a = k'a'\left(1 - \frac{q}{q_\infty}\right) \tag{10}$$

Consequently its mass balance in the medium becomes:

$$\frac{dq}{dt} = \frac{k'a'}{w}\left(1 - \frac{q}{q_\infty}\right)(1-\varepsilon)VC_s \tag{11}$$

where a′, w, q, and q_∞ are adsorption area per unit volume of medium, medium mass, adsorbed pollutant mass per unit mass of medium, and pollutant mass adsorbed in equilibrium with that in the aqueous film per unit mass of the medium, respectively.

As the medium becomes gradually saturated by organic pollutants at a certain height, the concentration of organic pollutants in the waste gas stream that passes through there may be assumed to reach the state of equilibrium in a much slower time scale than that in an aqueous layer (*i.e.*, C_l) does. In this manner one may assume that q and q_∞ also behave on a slower time scale.

Substituting Eq. (10) for k_a into the expression of α from Eq. (4) to apply the clouding effect, one gets:

$$\alpha = \Lambda\left(1-\frac{q}{q_\infty}\right) \text{ where } \Lambda = \frac{k'a'(1-\varepsilon)}{D_e a} \tag{12}$$

and one may assume that α varies in a slower manner like q does, than such a variable as C_l in the aqueous film does. The quasi-steady state of the mass balance in the aqueous film is then assumed and its quasi steady state solution is available where α is expressed by use of process-lumping model parameter (Λ) as in Eq. (12). From its quasi-steady-state solution one gets quasi-steady state diffusion flux at the interface between the aqueous film and the sorption volume of the medium, and may substitute it into N from the mass balance of organic pollutants in the gas phase of an adsorption column (*i.e.*, Eq. (13)).

$$\varepsilon\frac{\partial C_g}{\partial t} + u\frac{\partial C_g}{\partial h} = -Na \tag{13}$$

where N may be replaced with Eq. (8).

The pollutant mass adsorbed per unit mass of the medium in equilibrium with that dissoved in the aqueous film (q_∞), is assumed to be $KC_l^{1/n}(\sigma=1)$ according to a Freundlich adsorption isotherm. It is substituted in Eq. (12). Then one gets

$$q = \left(1-\frac{\alpha}{\Lambda}\right)K\left[\frac{C_g/m}{(1+\alpha l)}\right]^{1/n} \tag{14}$$

Eq. (4), that is the boundary condition at $x=l$ of the mass balance in the aqueous film (Eq. (1)), is substituted into the mass balance of the adsorbed pollutant mass per unit mass of the medium (Eq. (15), q, as below:

$$\frac{\partial q}{\partial t} = -D_e\frac{\partial C_l}{\partial x}\bigg|_{x=l} a(V/w) \tag{15}$$

One gets:

$$\frac{\partial q}{\partial t} = \frac{(C_g/m)D_e a(V/w)\alpha}{(1+\alpha l)} \tag{16}$$

4. Numerically Integrated Solution

Applying the values of the model parameters from dynamic adsorption column experiments as well as adsorption isotherm, a time-varying pollutant concentration of treated waste air may be obtainable by numerical integration with the aid of the unsteady mass balance of C_g along the height of adsorption column (Eq. (13)) and unsteady mass balance of q (Eq. (16)), and the definition of α that relates q to C_g (Eq. (14). To solve the set of partial differential equations and an algebraic equation the subroutine of DMOLCH from IMSL 32-Bit Fortran Numerical Libraries 3.0 with Fortran Power Station Compiler was used to apply the collocation approximation to the differential equations. According to the orthogonal collocation method, the coefficients of the approximation are obtained so that the trial solution satisfies the differential equation at the two Gaussian points in each subinterval where the trial solution is expanded in the series of Cubic Hermite polynomials for space-variable approximation.

RESULTS AND DISCUSSION

1. Model Prediction for the Dynamic Adsorption Behavior and Estimation of Process Lumping Constant (Λ) and Dynamic Adsorption Capacity (K)

Their dynamic adsorption behaviors were observed until they reached isothermal adsorption equilibrium, as shown in Figs. 3 and 4, at the position of feed inlet and three sampling ports of the adsorption columns when the first and second adsorption experiments were run for 160 and 80 hrs, respectively. The characteristics of the media packed in the adsorption column and used for adsorption isotherm experiments are shown in Table 1. The adsorption capacity parameters (K) and adsorption exponents (1/n) of the Freundlich adsorption isotherm were quantified statistically by linear regression (R^2=0.9975) from the log-scaled adsorption isotherm of a separate static batch experiment, and turned out to be, for sterilized equal volume mixture of GAC and compost, 5.243×10^{-6} (mg-ethanol/mg-media)/(mg-ethanol/m^3)$^{0.5688}$ and 0.5688, respectively [21]. To estimate the value of process-lumping model parameter (Λ) the dynamic adsorption behavior of the column fed with 4,100 mg ethanol/m^3 (or 2,000 ppmv)-ethanol vapor was predicted as the para-

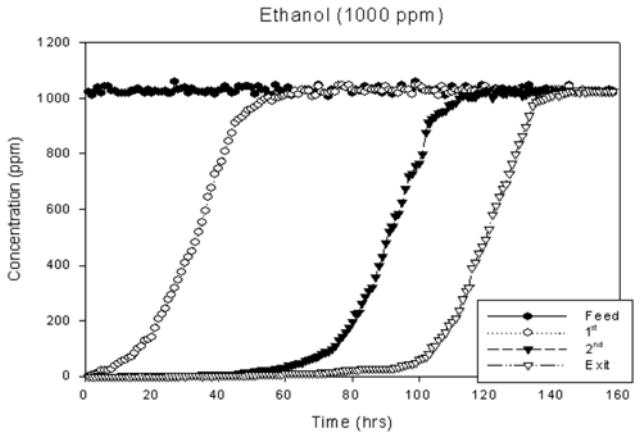

Fig. 3. Time evolutions of ethanol concentrations of the adsorption experiment at each sampling port of an adsorption column fed with waste air (2 L/min) containing ethanol of 1,000 ppmv (or 2,050 mg ethanol/m^3) [22]: (a) 1st (ζ=0.3); (b) 2nd (ζ=0.8); (c) Exit (ζ=1.0). [ζ: dimensionless height coordinates of adsorption column].

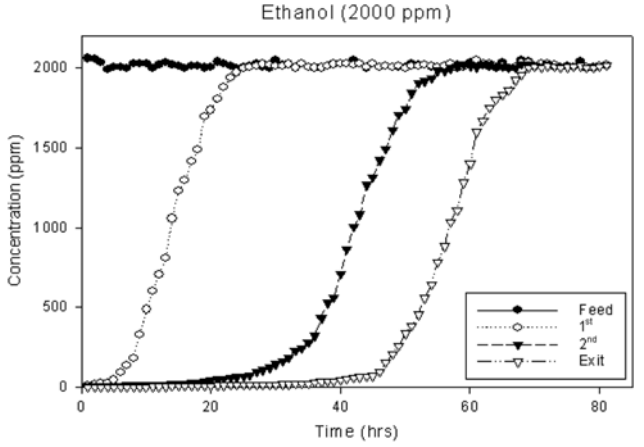

Fig. 4. Time evolutions of ethanol concentrations of the adsorption experiment at each sampling port of an adsorption column fed with waste air (2 L/min) containing ethanol of 2,000 ppmv (or 4,100 mg ethanol/m^3) [22]: (a) 1st (ζ=0.3); (b) 2nd (ζ=0.8); (c) Exit (ζ=1.0). [ζ: dimensionless height coordinates of adsorption column].

metric sensitivity with various value of process-lumping model parameter (Λ) using the set of the values of the obtained Freundlich adsorption isotherm parameters, as shown in Figs. 5(a)-(c). Moreover, the experimental breakthrough curve at the exit of Fig. 4 is also shown in Figs. 5(a)-(c) (white diamond symbols) with the conversion of units. The onset of breakthrough was predicted to be delayed as the value of process lumping model parameter (Λ) increased from 16.7/m to 50.1/m, as shown in Figs. 5(a)-(c). Among those predictions, the onset of breakthrough of the 5% feed concentration at the exit of the adsorption column for the value of the process lumping constant (Λ) of 33.4/m, was found to be qualitatively the most similar to the corresponding experimental result with an ethanol-feed concentration of 4,100 mg ethanol/m^3 (or 2,000 ppmv). Nevertheless, compared to the corresponding experimental result at the exit of the adsorption column with the ethanol-feed concentration of 4,100 mg ethanol/m^3 (or 2,000 ppmv), 1) the most similar prediction (Fig. 5(b)) was observed to have a delayed onset of breakthrough of 5% feed concentration at the exit; 2) the onset of reaching the state of dynamic equilibrium at the exit was much longer delayed for all the above tried ranges of Λ in Fig. 5(a)-(c). This is because the adsorption capacity parameter (K) value of the Freundlich adsorption

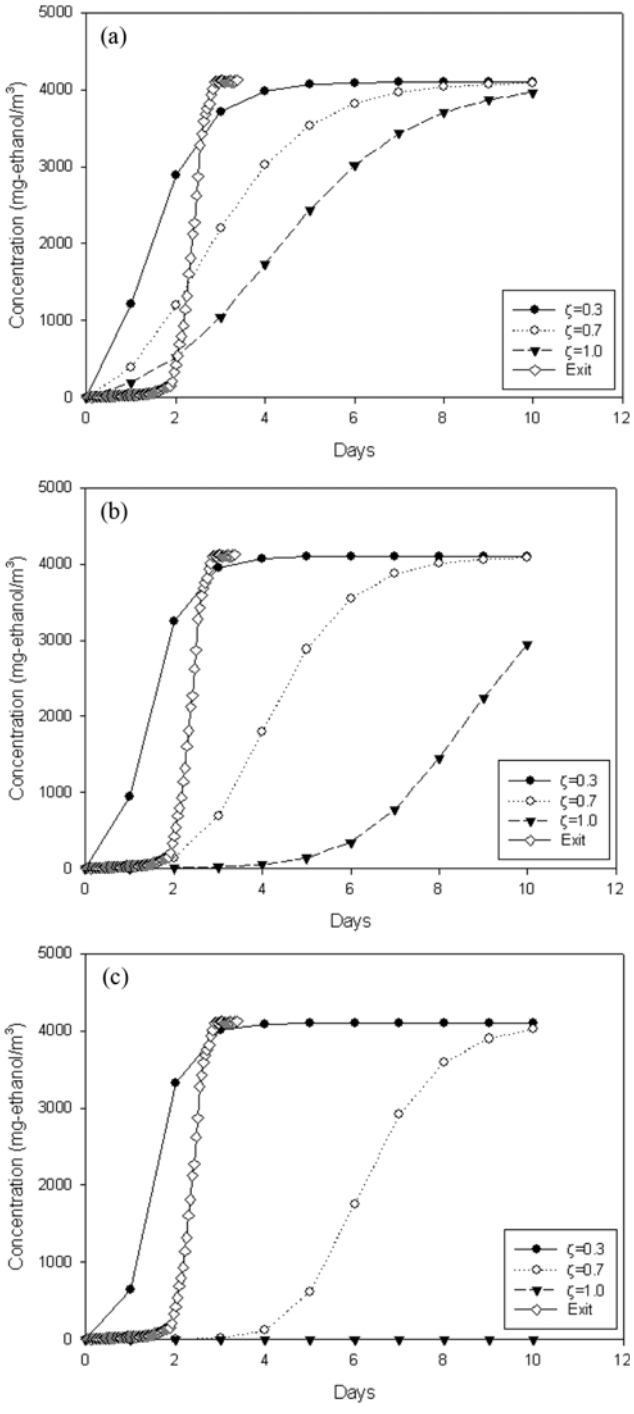

Fig. 5. Parametric sensitivity of the unsteady treated-ethanol concentration predicted at three different dimensionless height of an adsorption column (ζ=0.3, 0.7 and 1.0) with respect to the process-lumping parameter (Λ) using the model parameters from Table 2, and the experimental breakthrough curve (◇) at the exit of an adsorption column fed with waste air (2 L/min) containing ethanol of 4,100 mg ethanol/m^3 (or 2,000 ppmv): (a) Λ=16.7/m; (b) Λ=33.4/m; (c) Λ=50.1/m.

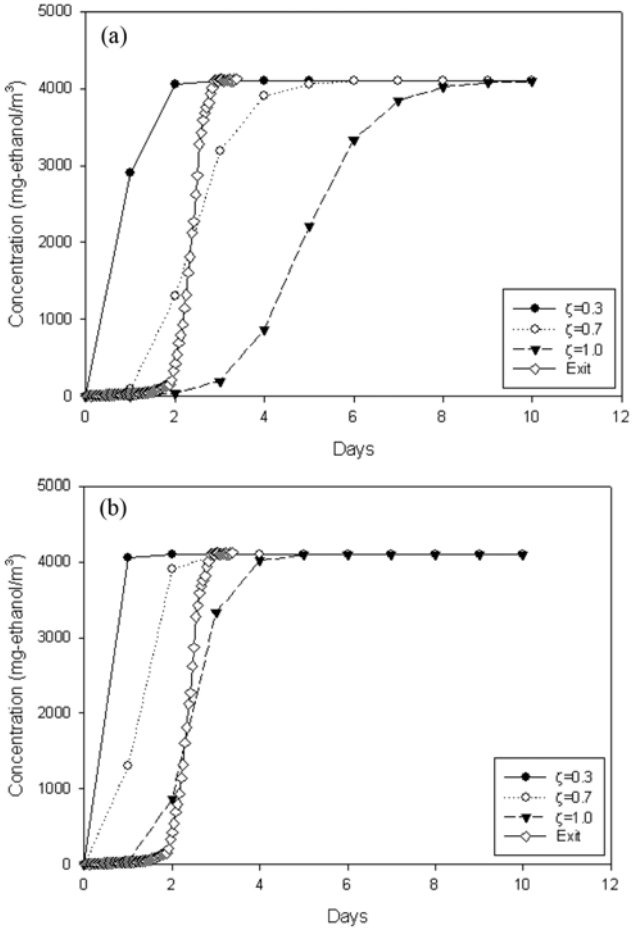

Fig. 6. Parametric sensitivity of the unsteady treated-ethanol concentration at three different dimensionless height of an adsorption column (ζ=0.3, 0.7 and 1.0) with respect to K, using the model-prediction with model parameters from Table 2 except for K, and the experimental breakthrough curve (◇) at the exit of an adsorption column fed with waste air (2 L/min) containing ethanol of 4,100 mg ethanol/m^3 (or 2,000 ppmv): (a) Λ=33.4/m, K=2.622×10^{-6} (mg-ethanol/mg-media)/(mg-ethanol/m^3)$^{0.5688}$; (b) Λ=33.4/m, K=1.311×10^{-6} (mg-ethanol/mg-media)/(mg-ethanol/m^3)$^{0.5688}$.

Table 2. Model parameter values

K	5.243×10^{-6} (mg-ethanol/mg-media)/(mg-ethanol/m^3)$^{0.5688}$	[21]
1/n	0.5688	[21]
a	2136 m^2/m^3	[Table 1]
D_e	10^{-9} m^2/s	[26]
H	0.44 m	[22]
l	10^{-4} m	[6]
V/w	2.69×10^{-9} m^3/mg	[22]
m	0.0003	[21]

isotherm available by static batch method may exceed that from dynamic continuous flow-adsorption experiments, due to the hydrodynamic condition of a gas phase feed flow and the possible existence of dead zone caused by the channeling of hydrodynamic flow in an actual adsorption column for dynamic continuous-adsorption experiments. It is supported by the experimental evidence, reported by Kant and Rattan [27], saying that adsorption is better in a batch process in respect to the continuous flow method. Therefore, the dynamic-continuous flow-adsorption behavioral value of adsorption capacity parameter (K) may be set to be one-half or one-quarter of the value (5.243×10^{-6} (mg-ethanol/mg-media)/(mg-ethanol/m^3)$^{0.5688}$) previously determined by the static batch method. Then their dynamic adsorption behaviors were predicted as a parametric sensitivity with respect to K as shown in Figs. 6(a) and (b), respectively. Besides, the experimental breakthrough curve at the exit of Fig. 4 is also shown in Figs. 6(a)-(b) (white diamond symbols) with the conversion of units. The onset of reaching the state of equilibrium was predicted closer to the experimental data in Fig. 6(b) than in Fig. 6(a). The proposed dynamic adsorption model-fit is predicted with the model-fit parameter values including the 25%-increased value of Λ (Table 3), as shown in Fig. 7, to compensate for the advanced onset of breakthrough at the exit of Fig. 6(b). In addition, the experimental results of Fig. 4 are also shown in Fig. 7 (gray symbols) with the conversion of units. As a result, the dynamic adsorption behavior was predicted corresponding to the result of dynamic adsorption experiment with the ethanol-feed concentration of 4,100 mg ethanol/m^3 (or 2,000 ppmv). Figs. 8(a) through e show the parametric sensitivity of the dynamic adsorption column behavior at three different dimensionless height of an adsorption column (ζ=0.3, 0.7 and 1.0) with respect to the adsorption exponents (1/n) of the Freundlich adsorption isotherm, keeping the set of model-fit adsorption model parameters (Table 3) except for the adsorption exponents (1/n). The values of the adsorption exponents (1/n) varied from

Table 3. Model-fit parameter values

K	1.311×10^{-6} (mg-ethanol/mg-media)/(mg-ethanol/m^3)$^{0.5688}$	[This study]
1/n	0.5688	[21]
a	2136 m^2/m^3	[Table 1]
D_e	10^{-9} m^2/s	[26]
H	0.44 m	[22]
l	10^{-4} m	[6]
V/w	2.69×10^{-9} m^3/mg	[22]
m	0.0003	[21]
Λ	41.8/m	[This study]

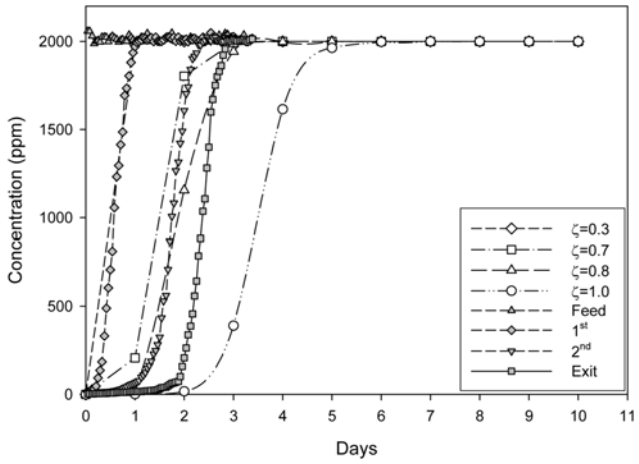

Fig. 7. Adsorption model-prediction (white) with model-fit parameter values from Table 3 vs. Time evolutions of ethanol concentrations (gray) of the adsorption experiment at each sampling port of an adsorption column fed with waste air (2 L/min) containing ethanol of 2,000 ppmv (or 4,100 mg ethanol/m^3) [22]: (a) 1st (ζ=0.3); (b) 2nd (ζ=0.8); (c) Exit (ζ=1.0).

0.4 to 0.9 in Figs. 8(a)-(e). As the values of the adsorption exponents (1/n) increased, the onset of breakthrough was generally delayed.

2. Model Validation of Dynamic Adsorption Behavior

With the set of adsorption model-fit parameter values (Table 3), the dynamic adsorption model was validated for the ethanol-feed concentration of 2,050 mg ethanol/m^3 (or 1,000 ppmv) as shown in Fig. 9. In addition, the experimental results of Fig. 3 are also shown in Fig. 9 (gray symbols) with the conversion of units. The model-validated onsets of reaching the state of dynamic equilibrium at the position of ζ=0.3 (first sampling port) and 1.0 (exit) of the adsorption column correspond to the second and seventh days, respectively, of the adsorption column run, which is consistent with those of the dynamic adsorption experiment. In the dynamic adsorption experiments, the first and second sampling ports, and the exit were positioned unequal distance apart at ζ=0.3, 0.8 and 1.0, respectively. Such an allocation-limit of sampling port position was caused by the use of the same tubes for upper and lower reactor tubes of real adsorption column. For its compensation, the dynamic adsorption behavior of the proposed adsorption model was predicted at the more equally distanced positions of ζ=0.3, 0.7, 0.8 and 1.0. In the dynamic adsorption model-fit with the ethanol-feed concentration of 4,100 mg ethanol/m^3 (or 2,000 ppmv), of Fig. 7, the model-predicted breakthrough at ζ=0.7 comes sooner by a quarter of a day than the model-predicted breakthrough (ζ=0.8) as well as the experimental breakthrough at second sampling port (ζ=0.8). However, in the dynamic model-validation for the ethanol-feed concentration of 2,050 mg ethanol/m^3 (or 1,000 ppmv) as shown in Fig. 9, the time-lag of predicted breakthroughs between ζ=0.7 and 0.8 increases to be longer than that as shown in Fig. 7.

CONCLUSIONS

We have proposed a dynamic adsorption model using the lumping process for an adsorption system. It was operated under the con-

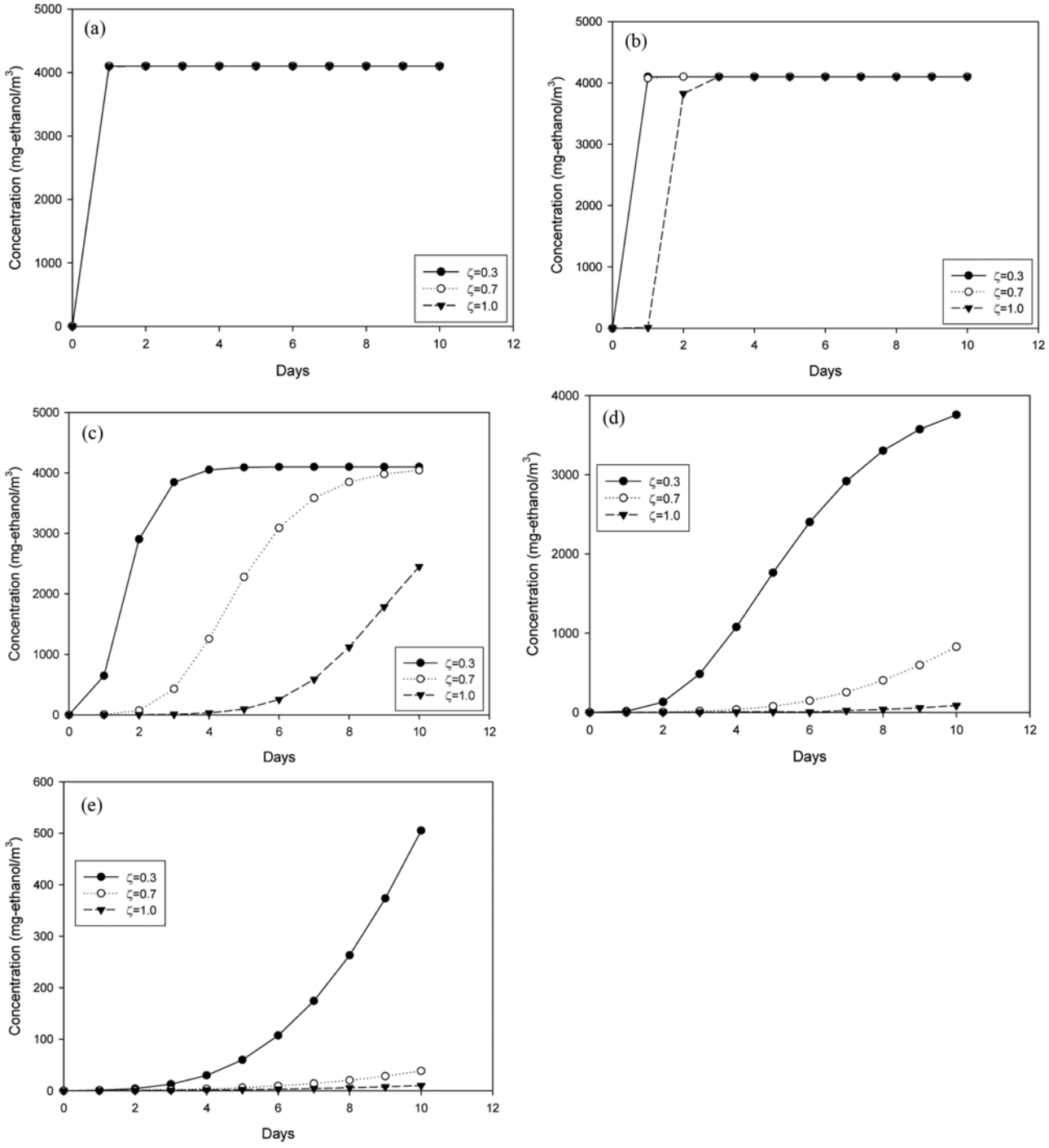

Fig. 8. Parametric sensitivity of the unsteady treated-ethanol concentration at three different dimensionless height of an adsorption column (ζ=0.3, 0.7 and 1.0) with respect to 1/n, using the model-prediction with model parameters except for 1/n, from Table 3 of an adsorption column fed with waste air (2 L/min) containing ethanol of 4,100 mg ethanol/m^3 (or 2,000 ppmv): (a) 1/n=0.4; (b) 1/n=0.5; (c) 1/n=0.7; (d) 1/n=0.8; (e) 1/n=0.9.

dition of almost saturated relative humidity of waste air fed to a biofilter, to treat waste air containing such a VOC as ethanol. It is meaningful that the suggested dynamic adsorption model is the novel one that consists of four components: gas phase, enclosed aqueous phase, sorption volume and surface adsorption in the pore of media. The clouding effect in k_a was adopted to explain an actual adsorption process in which its adsorption capacity is limited as adsorption sites on the surface of medium are occupied. In the equilibrium stage the Freundlich adsorption isotherm was adopted. To estimate the adsorption model parameter values in a biofilter fed with ethanol at 4,100 mg ethanol/m^3 (or 2,000 ppmv), the proposed adsorption model was predicted in comparison with the experimental values of an adsorption column. The dynamic-continuous flow-adsorption behavioral value of adsorption capacity parameter (K) was chosen

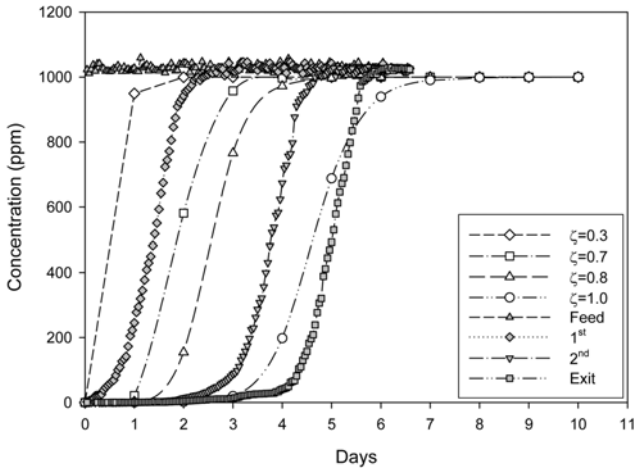

Fig. 9. Adsorption model validation (white) with model-fit parameter values from Table 3 vs. Time evolutions of ethanol concentrations (gray) of the adsorption experiment at each sampling port of an adsorption column fed with waste air (2 L/min) containing ethanol of 1,000 ppmv (or 2,050 mg ethanol/m^3) [22]: (a) 1st (ζ=0.3); (b) 2nd (ζ=0.8); (c) Exit (ζ= 1.0).

to be set at one-quarter of the value previously determined by a static batch method. It was consistent with the experimental evidence reported by Kant and Rattan, saying that adsorption was better in a batch process in respect to the continuous flow method. With the set of chosen adsorption model parameter values, the dynamic adsorption model was validated for the ethanol-feed concentration of 2,050 mg ethanol/m^3 (or 1,000 ppmv). The model-fit values of the Freundlich adsorption isotherm constants were obtained statistically by linear regression from the adsorption isotherm of a separate static batch experiment. However, in this study, the model-fit values of the proposed model parameters, except for those of the Freundlich adsorption isotherm, were not determined by a curve-fitting technique such as nonlinear regression, which frequently leads their cost function to be caught at its meaningless local minima instead of the global minimum of their cost function. To the best of our knowledge no one has used nonlinear regression to estimate the model parameters for the unsteady biofilter model due to tremendous CPU time to statistically perform nonlinear regression requiring huge number of simultaneous integration of the set of coupled unsteady partial differential equations of biofilter model-governing equations. Instead, the undetermined values of model-fit parameters have been very often chosen among the parameter values used for a parametric sensitivity analysis to be close to the experimental data of unsteady biofilter-runs. In this way they were obtained qualitatively upon analyzing mechanistically the parametric sensitivity of the suggested dynamic adsorption model. Since process lumping constant (Λ) contains the expression of initial adsorption rate, it functions primarily on the onset of a breakthrough from its curve. We analyzed the parametric sensitivity of the unsteady treated-ethanol concentration at three different dimensionless heights of an adsorption column (ζ= 0.3, 0.7 and 1.0) with respect to the process-lumping parameter (Λ). Accordingly, the fitting value of process lumping constant (Λ) was chosen in comparison with the onset of breakthrough from the corresponding experimental data. Then it was followed by the adjustment on adsorption capacity parameter (K) value of Freundlich adsorption isotherm according to its parametric sensitivity analysis to be closer to the experimental data. Nevertheless, results showed that the mechanistic model was able to simulate the dynamic behavior of an adsorption process successfully according to the corresponding adsorption experimental data.

ACKNOWLEDGEMENT

This research was financially supported by the Ministry of Education, Science Technology (MEST) and National Research Foundation of Korea (NRF) through the Human Resource Training Project for Regional Innovation.

NOMENCLATURE

a : interfacial area per unit volume of the medium [m^2/m^3]
C_g : concentration in the gas phase [mg/m^3]
C_{go} : inlet concentration in the gas phase [mg/m^3]
C_l : concentration in the aqueous film [mg/m^3]
C_s : concentration in the aqueous phase of the sorption volume [mg/m^3]
D_e : diffusion coefficient in the aqueous film [m^2/sec]
D_s : coefficient of surface diffusion [m^2/sec]
H : bed height of an adsorption column [m]
h : height coordinate of an adsorption column [m]
k_a : adsorption rate constant with excess adsorption capacity [sec^{-1}]
K, 1/n : Freundlich adsorption isotherm constants
l : aqueous film thickness [m]
m : distribution coefficient between the gas phase and the aqueous film
N : diffusive flux at the interface between the gas phase and the aqueous film [mg/m^2·sec]
q : adsorbed substrate mass per unit mass of the medium [mg/mg-media]
u : approach velocity of a waste gas stream [m/sec]
V : bed volume of an adsorption column [m^3]
$V_{sorption}$: sorption volume [m^3]
x : depth coordinate of the aqueous film [m]
α : ratio of ka$(1-\varepsilon)$ to D_ea [m^{-1}]
ε : bed porosity
σ : dimensionless depth coordinate of the aqueous film
ζ : dimensionless height coordinates of an adsorption column

REFERENCES

1. B. E. Bittman and P. L. McCarty, *Biotechnol. Bioeng.*, **22**, 2343 (1980).
2. B. E. Bittman and P. L. McCarty, *Biotechnol. Bioeng.*, **22**, 2359 (1980).
3. S. P. P. Ottengraf, in *Biotechnology*, H. J., Rehm and G. Reed, Eds., **8**, 426-452, VCH, Weinheim, Germany (1986).
4. S. P. P. Ottengraf, J. J. P. Meesters, A. H. C. Van Den Oever and H. R. Rozema, *Bioprogress Eng.*, **1**(1), 61 (1986).
5. M. Hirai, M. Ohtake and M. Shoda, *J. Ferment. Bioeng.*, **70**, 334 (1990).
6. Z. Shareefdeen, B. C. Baltzis, Y. S. Oh and R. Bartha, *Biotechnol.*

Bioeng., **41**, 512 (1993).
7. M. A. Deshusses and G. Hamer, *Bioprocess Eng.*, **9**, 141 (1993).
8. M. A. Deshusses, G. Hamer and I. J. Dunn, *Environ. Sci. Technol.*, **29**, 1048 (1995).
9. G. E. Speitel, Jr. and D. S. Mclay, *J. Environ. Eng.*, **119**, 658 (1993).
10. S. Zarook and B. C. Baltzis, *Chem. Eng. Sci.*, **49**(24A), 4347 (1994).
11. S. M. Zarook, A. A. Shaikh and Z. Ansar, *Chem. Eng. Sci.*, **52**(5), 759 (1997).
12. Md. Amanullah, S. Farooq and S. Viswanathan, *Ind. Eng. Chem. Res.*, **38**(7), 2765 (1999).
13. C. Alonso, X. Zhu, M. T. Suidan, B. R. Kim and B. J. Kim, *J. Environ. Eng.*, **127**, 655 (2001).
14. H. Jorio, B. Payre and M. Heitz, *J. Chem. Technol. Biotechnol.*, **78**, 834 (2003).
15. A. H. Wani, R. M. R. Branion and A. K. Lau, *J. Environ. Sci. Health*, **A32**, 2027 (1997).
16. V. J. Lith, *Air & Waste Mgmt. Assoc.*, **47**, 37 (1997).
17. R. Auria, A. C. Aycagner and J. S. Devinny, *J. Air & Waste Mgmt. Assoc.*, **48**, 65 (1997).
18. A. Joly and A. Perrard, *Mathematics and Computers in Simulation*, **79**, 3492 (2009).
19. M. Gholami, M. R. Talaie and S. Roodpeyma, *Chem. Eng. Sci.*, **65**, 5942 (2010).
20. X. Zhang, X. Zhao, J. Hu, C. Wei and H. T. Bi, *J. Hazard. Mater.*, **186**, 1816 (2011).
21. E. J. Lee and K.-H. Lim, *Korean Chem. Eng. Res.*, **46**(5), 994 (2008).
22. E. J. Lee, K. S. Seo, W. S. Jeon and K.-H. Lim, *Korean Chem. Eng. Res.*, **50**(1), 149 (2012).
23. D. W. Hand, J. C. Crittenden and W. E. Thacker, *J. Environ. Eng.*, **109**(1), 82 (1983).
24. G. E. Speitel, Jr., K. Dovantzis and F. A. DiGiano, *J. Environ. Eng.*, **113**(1), 32 (1987).
25. G E. Speitel, Jr. and F. A. DiGiano, *J. Am. Water Works Assoc.*, **79**(1), 64 (1987).
26. R. H. Perry and D. Green, Perry Chemical Engineers' Handbook, 6th Ed. (1987).
27. R. Kant and V. K. Rattan, *Indian J. Chem. Technol.*, **16**, 240 (2009).